Nonlinear Dyn (2009) 57: 623–633
DOI 10.1007/s11071-009-9502-3

ORIGINAL PAPER

Resonant dynamics in a rotordynamic system with nonlinear inertial coupling and shaft anisotropy

D. Dane Quinn

Received: 29 August 2008 / Accepted: 30 March 2009 / Published online: 15 April 2009

Abstract The response of a nonlinear, damped Jeffcott rotor with anisotropic stiffness is considered in the presence of an imbalance. For sufficiently small external torque or large imbalance, resonance capture or rotordynamic stall can occur, whereby the rotational velocity of the shaft is unable to increase beyond the fundamental resonance between the rotational and translational motion. This phenomena provides a mechanism for energy transfer from the rotational to the translational mode. Using the method of averaging a reduced-order model is developed, valid near the resonance, that describes this resonant behavior. The equilibrium points of these averaged equations, which correspond to stationary solutions of the original equations and rotordynamic stall, are described as the applied torque, damping, and anisotropy vary. As the anisotropy increases, assumed to arise from increasing shaft cracks, the torque required to eliminate the possibility of stall increases. However, when the system is started with zero initial conditions, the minimum torque required to pass through the resonance is approximately constant as the anisotropy increases. The predictions from the reduced-order model are verified against numerical simulations of the original equations of motion.

D.D. Quinn (✉)
Department of Mechanical Engineering,
The University of Akron, Akron, OH 44325–3903, USA
e-mail: quinn@uakron.edu

Keywords Resonance capture · Non-ideal system · Rotordynamic imbalance

1 Introduction

The amplified response of unbalanced rotordynamic systems near their critical speeds can be associated with the resonance that exists between the rotational speed of the rotor and the oscillation frequency of the translational dynamics. The resonance can serve to enhance the coupling between components and/or vibrational modes, and this coupling can often lead to dramatic, undesirable changes in the performance of the system at hand. One such example occurs when rotordynamic systems are driven through a critical speed [1–3]. This passage through resonance is often accompanied by an increase in the vibrational amplitudes of the system and an increase in the power required to maintain a specified acceleration rate.

For certain operational characteristics, most notably for sufficiently large torques and/or damping, this behavior does not occur. Instead, the system responds similar to that of the balanced system, which has no coupling between translational and rotational motions. However, if the external excitation is only capable of limited torque and/or power, the rotating system may be unable to pass through the critical speed. Instead, it may be captured into resonance [4–6]. That is, because of the inertial coupling present between the

translational and rotational dynamics due to the imbalance, on average the angular velocity of the rotor remains constant, near the vibrational frequency of the shaft. The energy input to the system from the external torque is transmitted to the translational oscillations, which may increase to unacceptably large amplitudes.

Previous work [6–10] has focused on this effect in system with only rotating imbalance. In the present work the response of an unbalanced rotating shaft with anisotropic stiffness is considered. The anisotropy is assumed to arise from a shaft crack and induces a fluctuating stiffness in the system. Thus we consider equations of motion describing the displacement of the rotor coupled to an equation governing the rotational motion of the shaft. Using the method of averaging these equations are reduced near the resonant behavior and the parameter values that lead to this resonant behavior are delineated. Finally, it is noted that the failure of the system to pass through resonance depends on not only the parameter values but the initial conditions as well. As the system approaches the resonant conditions, capture requires that there is sufficient energy in the translational oscillations. Finally, a recent work by Samantaray [11] has focused on the stationary response of a similar shaft–rotor system.

2 Model

2.1 Equations of motion

Following Gasch [12], we consider a Jeffcott rotor model with the inclusion of mass imbalance in the presence of a transverse crack in the shaft. The crack is phenomenologically represented by an anisotropic shaft stiffness whose magnitude is assumed to be related to the depth of the crack, although no attempt is made in this paper to identify a constitutive relations between the crack depth and change in shaft stiffness. Rather, the stiffness anisotropy is assumed to be an independent parameter. As shown in Fig. 1, the displacement of the rotor center is $\mathbf{u}(t) = z\hat{\boldsymbol{k}} + x\hat{\boldsymbol{\imath}}$ while the rotation of the shaft is measured by the angle θ—if the location of the mass imbalance is defined as $\mathbf{r}_{GC} = \sigma\hat{\boldsymbol{k}}_2$, the angle between $\hat{\boldsymbol{k}}$ and $\hat{\boldsymbol{k}}_2$ is identified as θ. Finally, the angle γ represents the angle between the mass center ($\hat{\boldsymbol{k}}_2$) and $\hat{\boldsymbol{e}}_\xi$, the direction normal to the crack face. For the sake of brevity, the dimensional equations are not presented.

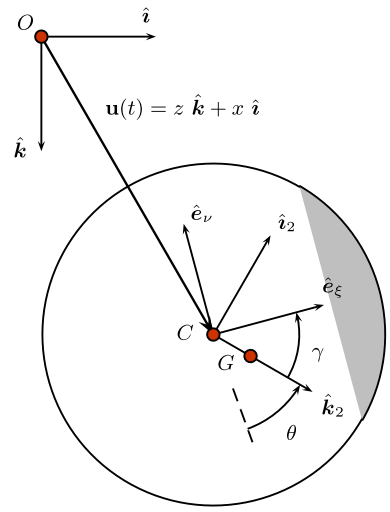

Fig. 1 Crack cross-sectional coordinates and directions

The nondimensional equations of motion for a simple rotor with a cracked shaft can be written in a stationary frame of reference as [12, 13]

$$\ddot{z} + 2(e\zeta)\dot{z} + z = d + e\Big\{\rho\big(\dot{\theta}^2\cos\theta + \ddot{\theta}\sin\theta\big) + \kappa f(\vartheta) \times \Big[z + \delta\big(z\cos\big(2(\theta+\gamma)\big) + x\sin\big(2(\theta+\gamma)\big)\big)\Big]\Big\}, \tag{1a}$$

$$\ddot{x} + 2(e\zeta)\dot{x} + x = e\Big\{\rho\big(\dot{\theta}^2\sin\theta - \ddot{\theta}\cos\theta\big) + \kappa f(\vartheta) \times \Big[x + \delta\big(z\sin\big(2(\theta+\gamma)\big) - x\cos\big(2(\theta+\gamma)\big)\big)\Big]\Big\}, \tag{1b}$$

$$\ddot{\theta} = e\big\{T(\dot{\theta}) + \rho(\ddot{z}\sin\theta - \ddot{x}\cos\theta) - \rho d\sin\theta\big\}. \tag{1c}$$

Time has been scaled by the shaft oscillation frequency while the displacements have been scaled by the radius of gyration of the disk. In this system d represents the (nondimensional) static displacement due to gravity. The magnitude of the imbalance is represented by $e\rho$, while $e\zeta$ is the damping ratio of the translational oscillations. The nondimensional torque is $eT(\dot{\theta})$, describing a non-ideal system with limited power supply, so that the applied torque to the rotor depends explicitly on its rotational speed. Here the parameter e is simply a scaling parameter introduced for convenience in the perturbation analysis be-

low. The crack steering function $f(\vartheta)$ describes the change in stiffness with shaft rotation on the stiffness due to the opening and closing of the crack with $\vartheta = \theta + \gamma - \arctan(x/z)$. Finally, κ and δ characterize the magnitude of the stiffness variations induced by the presence of the crack. If k_ξ and k_ν represent the shaft stiffness in the $\hat{\boldsymbol{e}}_\xi$ and $\hat{\boldsymbol{e}}_\nu$ directions respectively (see Fig. 1), then κ and δ are defined as

$$1 - e\kappa f(\vartheta) = \frac{k_\xi + k_\nu}{2}, \qquad -e\kappa\delta f(\vartheta) = \frac{k_\xi - k_\nu}{2}.$$

In what follows we assume that the crack is always open, so that $f(\vartheta) = 1$. This nonetheless leads to stiffness fluctuations that are correlated with the rotation of the shaft. A purely numerical investigation of these equations in the presence of a breathing crack, with $f(\vartheta) = (1 + \cos\vartheta)/2$, has been performed by Sawicki et al. [13].

Numerical simulations We numerically illustrate the dynamical behavior of (1). Unless noted, parameters take the following values

$$e\rho = 0.10, \quad eT = 0.0375, \quad e\zeta = 0.10,$$
$$e\kappa = 0.10, \quad \delta = 0.833, \quad \gamma = 0, \quad d = 0.10.$$

As seen in Fig. 2a, for this set of parameter values the system is captured into resonance. That is, the rotor stalls and its angular velocity cannot increase through the resonance with the translational motion. Note that the frequency at which the system is locked is not exactly equal to the translational natural frequency, here nondimensionalized to be unity. In contrast, as illustrated in Fig. 2b, as the nondimensional torque is increased to $eT = 0.050$ the angular velocity of the shaft passes through the resonance. Increasing the shaft anisotropy to $e\kappa = 0.20$ as shown in Fig. 2c, the system is again captured into resonance, and the amplitude of the translational oscillations increases compared to the simulation shown in Fig. 2a. Finally, as seen in Fig. 2d, as the damping parameter is increased to $e\zeta = 0.20$ (from the baseline parameters) the system passes through the resonance.

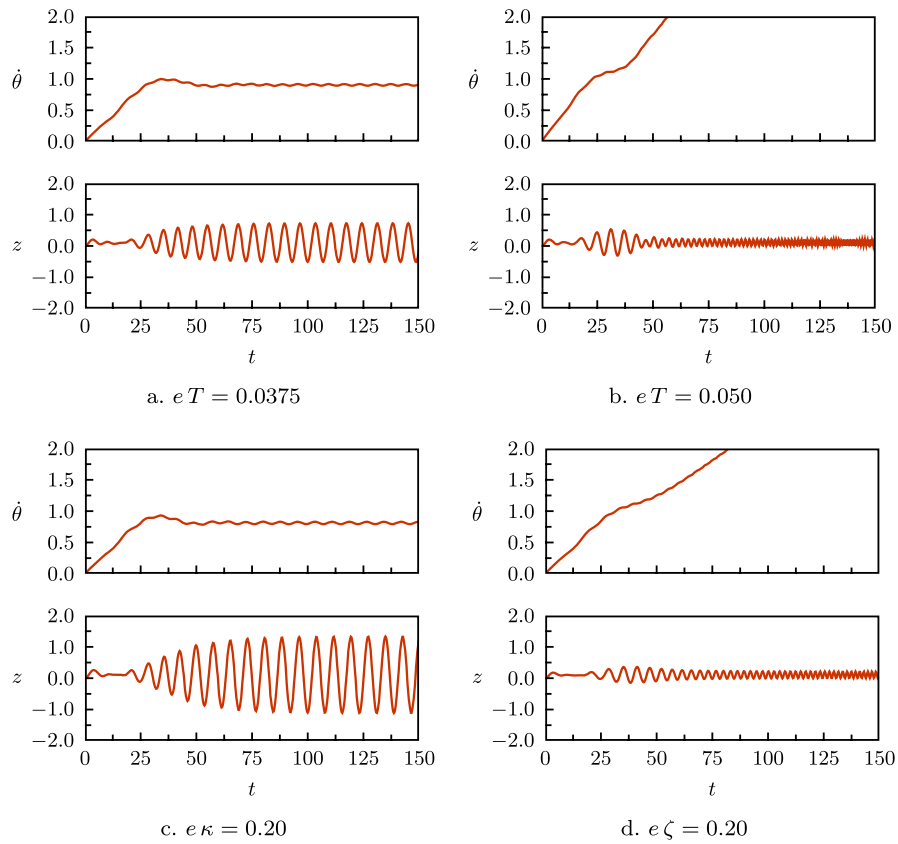

Fig. 2 Numerical simulation of (1). Unless noted, $e\rho = 0.10$, $eT = 0.0375$, $e\zeta = 0.10$, $e\kappa = 0.10$, $\delta = 0.833$, $\gamma = 0$, and $d = 0.10$. Each solution has zero initial conditions

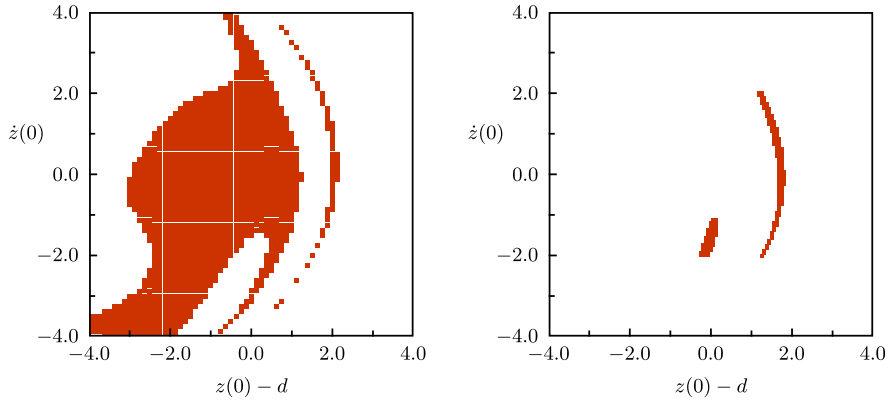

Fig. 3 Numerical simulation of (1) ($e\rho = 0.10$, $e\zeta = 0.10$, $e\kappa = 0.10$, $\delta = 0.833$, $\gamma = 0$, $d = 0.10$). Each marked initial condition leads to a solution that is captured into resonance

In addition to the above described dependence on the parametric values, the behavior of this system is also dependent on the initial conditions. In Fig. 3 the region of initial conditions that leads to a stalled solution is shown. The system was simulated with the initial conditions

$$x(0) = -\dot{z}(0), \qquad \dot{x}(0) = z(0) - d,$$
$$\theta(0) = 0, \qquad \dot{\theta}(0) = 0.$$

The initial conditions on $(x(0), \dot{x}(0))$ are chosen so that the x and z translational modes are out-of-phase by $\pi/2$ with identical amplitudes. As shown in Fig. 3 the initial conditions on $(z(0), \dot{z}(0))$ are varied over an $N \times N$ grid, here with $N = 64$. In each panel marked initial conditions correspond to solutions that fail to pass through the resonance. Notice that for $eT = 0.0375$ the region of initial conditions that lead to a captured solution is large and includes the origin (zero initial conditions, as shown in Fig. 2a). In contrast, for $eT = 0.050$ the capture region does not include the origin (cf. Fig. 2b). Nonetheless, for this value of the nondimensional torque there remain some initial conditions that stall and do not increase in angular velocity. However, as T is further increased (not shown), no initial conditions lead to a captured state.

3 Method of averaging

We study the dynamical behavior of (1) in the neighborhood of the resonance $\dot{\theta} = 1$ using the method of averaging. In preparation for averaging, we introduce the following polar coordinates

$$z(t) = d + r_1(t)\cos\phi_1(t), \qquad x(t) = r_2(t)\cos\phi_2(t),$$
$$\dot{z}(t) = r_1(t)\sin\phi_1(t), \qquad \dot{x}(t) = r_2(t)\sin\phi_2(t). \tag{2}$$

With these transformations, the equations of motion can be represented as

$$\dot{\phi}_1 = -1 + e g_{\phi_1}, \qquad \dot{\phi}_2 = -1 + e g_{\phi_2},$$
$$\dot{r}_1 = e g_{r_1}, \qquad \dot{r}_2 = e g_{r_2},$$
$$\dot{\theta} = \omega, \qquad \dot{\omega} = e g_{\omega},$$

where the functions $g_{(\bullet)}$ are easily obtained from (1). Note that the quantities r_1, r_2, and ω all vary slowly in time, while ϕ_1, ϕ_2, and θ are all angular variables. Away from the resonance ($\omega \sim 1$), the angular combinations $\psi_1 \equiv \phi_1 + \theta$ and $\psi_2 \equiv \phi_2 + \theta - \pi/2$ have an $\mathcal{O}(1)$ frequency

$$\dot{\psi}_1 = (\omega - 1) + \mathcal{O}(e),$$
$$\dot{\psi}_2 = (\omega - 1) + \mathcal{O}(e).$$

However, near the resonance, these terms evolve slowly. The method of averaging introduces a set of near-identity transformations, chosen to remove terms that are periodic with $\mathcal{O}(1)$ frequency from the resulting averaged equations. In addition, the rotational speed is expressed as

$$\omega(t) = 1 + \sqrt{e} w(t),$$

and the nondimensional applied torque $eT(\omega)$ can be expanded as

$$eT(\omega) = eT(1) + e^{3/2}\frac{dT}{d\omega}(1)w(t) + \mathcal{O}\big(e^2\big).$$

For convenience we define

$$\alpha_0 \equiv T(1), \qquad \alpha_1 \equiv \frac{dT}{d\omega}(1),$$

so that $e\alpha(w) = e(\alpha_0 + \sqrt{e}\alpha_1 w)$. Using the computer algebraic program Maple, the method of averaging is applied to (1), which reduce to

$$\frac{dp_1}{dt} = w + \frac{\varepsilon}{4}\Bigg\{\rho\bigg[\frac{\cos(p_1+p_2)}{r_1} + \frac{\cos(p_1-p_2)}{r_2}\bigg] + \kappa\bigg[2 + \frac{\delta}{2}\bigg(\frac{r_1^2+r_2^2}{r_1 r_2} + 2\cos(2p_2)\bigg) \times \cos\big(2(p_1+\gamma)\big)\bigg]\Bigg\}, \tag{3a}$$

$$\frac{dw}{dt} = \alpha_0 - \rho\bigg[\frac{r_1}{2}\sin(p_1+p_2) + \frac{r_2}{2}\sin(p_1-p_2)\bigg] + \varepsilon\alpha_1 w, \tag{3b}$$

$$\frac{dr_1}{dt} = \varepsilon\Bigg\{-\zeta r_1 + \rho\frac{\sin(p_1+p_2)}{2} + \frac{\kappa\delta}{4}\big[r_1\sin\big(2(p_1+\gamma+p_2)\big) + r_2\sin\big(2(p_1+\gamma)\big)\big]\Bigg\}, \tag{3c}$$

$$\frac{dr_2}{dt} = \varepsilon\Bigg\{-\zeta r_2 + \rho\frac{\sin(p_1-p_2)}{2} + \frac{\kappa\delta}{4}\big[r_1\sin\big(2(p_1+\gamma)\big) + r_2\sin\big(2(p_1+\gamma-p_2)\big)\big]\Bigg\}, \tag{3d}$$

$$\frac{dp_2}{dt} = \frac{\varepsilon}{4}\Bigg\{\rho\bigg[\frac{\cos(p_1+p_2)}{r_1} - \frac{\cos(p_1-p_2)}{r_2}\bigg] + \frac{\kappa\delta}{2}\bigg(\frac{r_2^2-r_1^2}{r_1 r_2}\cos\big(2(p_1+\gamma)\big) - 2\sin\big(2(p_1+\gamma)\big)\sin(2p_2)\bigg)\Bigg\}, \tag{3e}$$

with $\varepsilon = \sqrt{e}$. In these equations, time has been scaled by ε and

$$p_1 = \frac{\psi_1+\psi_2}{2}, \qquad p_2 = \frac{\psi_1-\psi_2}{2}.$$

While upon first observation, these equations may not appear simpler than the original unaveraged equations, note that the evolution of three of these states, r_1, r_2, and p_2, is $\mathcal{O}(\varepsilon)$. Thus, the resulting system can be described as a slowly-varying single-degree-of-freedom oscillator. Specifically, when $\varepsilon = 0$ the state variables (r_1, r_2, p_2) become stationary, and the remaining equations on (w, p_1) are equivalent to those describing the rotation of an undamped, forced pendulum.

3.1 Equilibria

Equilibrium points of the averaged equations can be identified with stationary solutions of the original equations of motion, that is, a solution whose vibration amplitudes are, on average, constant in time. These stationary solutions are identified with the failure of the system to pass through the resonance.

Undamaged shaft ($\kappa = 0$) In the absence of a shaft crack the equations describing the response within the resonant region reduce to

$$\frac{dp_1}{dt} = w + \frac{\varepsilon}{4}\Bigg\{\rho\bigg[\frac{\cos(p_1+p_2)}{r_1} + \frac{\cos(p_1-p_2)}{r_2}\bigg]\Bigg\}, \tag{4a}$$

$$\frac{dw}{dt} = \alpha_0 - \rho\bigg[\frac{r_1}{2}\sin(p_1+p_2) + \frac{r_2}{2}\sin(p_1-p_2)\bigg] + \varepsilon\{\alpha_1 w\}, \tag{4b}$$

$$\frac{dr_1}{dt} = \varepsilon\Bigg\{-\zeta r_1 + \rho\frac{\sin(p_1+p_2)}{2}\Bigg\}, \tag{4c}$$

$$\frac{dr_2}{dt} = \varepsilon\Bigg\{-\zeta r_2 + \rho\frac{\sin(p_1-p_2)}{2}\Bigg\}, \tag{4d}$$

$$\frac{dp_2}{dt} = \frac{\varepsilon}{4}\Bigg\{\rho\bigg[\frac{\cos(p_1+p_2)}{r_1} - \frac{\cos(p_1-p_2)}{r_2}\bigg]\Bigg\}. \tag{4e}$$

The equilibrium points of these averaged equations may be written in terms of $\alpha(w) \equiv \alpha_0 + \varepsilon\alpha_1 w$ as

$$r_{1,\mathrm{eq}} = r_{2,\mathrm{eq}} = \sqrt{\frac{\alpha(w_{\mathrm{eq}})}{2\zeta}},$$

$$w_{\mathrm{eq}} = \pm\varepsilon\sqrt{\frac{2\zeta}{\alpha(w_{\mathrm{eq}})} - \frac{4\zeta^2}{\rho^2}},$$

$$\sin(p_{1,\mathrm{eq}}) = \sqrt{\frac{2\zeta\alpha(w_{\mathrm{eq}})}{\rho^2}}, \qquad p_{2,\mathrm{eq}} = 0.$$

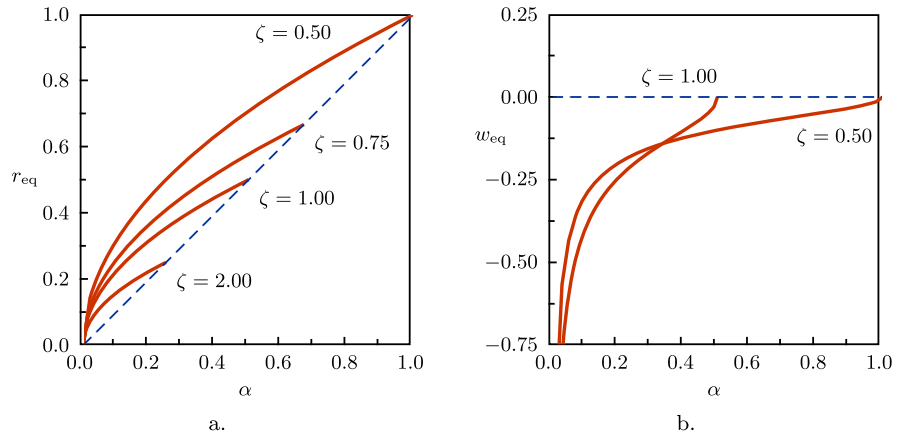

Fig. 4 Stable equilibria of the averaged equations for the undamaged shaft ($\varepsilon = 0.10$, $\rho = 1$, $\kappa = 0$, $\alpha_1 = 0$)

In this, $\alpha(w)$ represents the nondimensional external torque within the resonance region, so that $\alpha(w_{eq})$ is the external torque at the stationary state. Finally, the equation for w_{eq} may be simplified to

$$\varepsilon\alpha_1\rho^2 w_{eq}^3 + \big(\rho^2\alpha_0\big)w_{eq}^2 + \varepsilon\alpha_1(2\varepsilon\zeta)^2 w_{eq} - \varepsilon^2(2\zeta)\big(\rho^2 - 2\zeta\alpha_0\big) = 0. \tag{5}$$

This equation generically possesses either one or three solutions for ω_{eq}, depending on the parameter values. A matched asymptotic expansion for $\varepsilon \ll 1$ suggests these solutions exist near

$$w \sim -\frac{\alpha_0}{\varepsilon\alpha_1}, \quad \text{and} \quad w \sim \pm\varepsilon\sqrt{\frac{2\zeta}{\alpha_0} - \frac{4\zeta^2}{\rho^2}}.$$

The latter pair of equilibria, which only exist for specific parameter values, lie within the resonance region, while the former occurs for $|w_{eq}| \gg 1$, so that the stationary solution is far from the resonance. With $\alpha_1 < 0$, so that the external torque decreases with increasing speed, this additional solution is well above the resonance and corresponds to a solution that has passed through the resonance region.

Notice that for $\alpha_1 = 0$, so that the torque is independent of speed, the system predicts resonance capture occurs provided $2\zeta\alpha_0 < \rho^2$. This implies that if either the external torque or the damping is sufficiently small, resonance capture occurs for some initial conditions. With fixed damping, as the torque increases the amplitude of the translational vibrations increases as $\sqrt{\alpha_0}$, while the frequency at which the rotor becomes locked decreases with decreasing torque. As the damping decreases, stall occurs for a larger interval of external torques—the system requires more energy to pass through the resonance. The equilibrium that exists for $w_{eq} > 0$ is unstable, while the branch for $w_{eq} < 0$ is stable. In Fig. 4, these equilibria are shown as α_0 and ζ vary.

Many previous authors have focused on the speed–torque relationship, embodied with a nonzero α_1, as a critical component of resonance capture [10, 14]. However, as shown here, the presence of nonzero α_1 is not necessary for trajectories to become locked into resonance. Rather, it is the nonlinear coupling between the rotational and translational behavior that is responsible for this phenomena, identified as the "Sommerfield effect." Moreover, the effect of $\alpha_1 \neq 0$ on the behavior within the resonance region is small, provided $|\varepsilon\alpha_1| \ll 1$, although the speed–torque curves will ultimately limit the angular speed of trajectories that become locked into resonance, as evidenced by the persisting equilibrium in (5). We note that Bolla et al. [15] and El-Badawy [16] have recently considered systems with a single translational degree-of-freedom, as in Quinn et al. [6], finding reduced-order equations in the resonance region similar to the present work, as well as earlier efforts by Zniber and Quinn [17].

In the work of Bolla et al. [15] the parameter α_1 was effectively assumed to be $\mathcal{O}(1/\varepsilon)$, implying that the maximum allowable angular speed of the rotor was within the resonance region. However, if the external torque is chosen so that the balanced system is expected to reach angular speeds well above the resonance, then $\alpha_1 = \mathcal{O}(1)$. Consequently, the speed–torque characteristic with nonzero α_1 plays in general a small role in the near-resonant response. As described above, this effect only becomes significant when the expected angular speed obtained by solving for $\alpha(\omega) = 0$ approaches the resonant frequency at

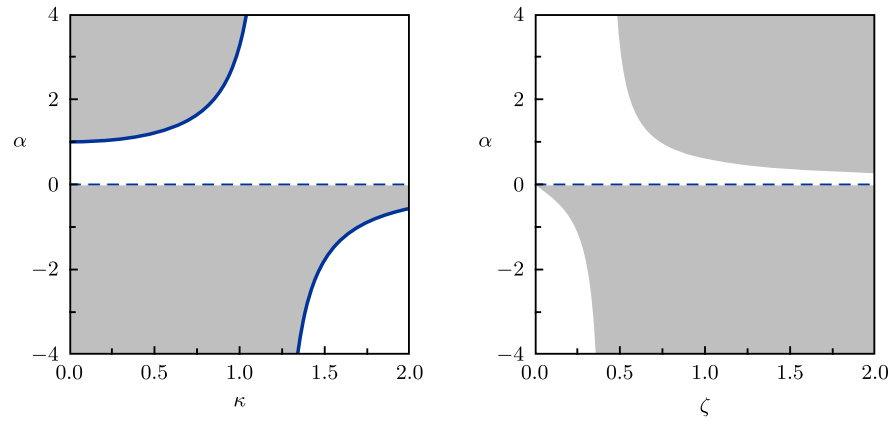

a. $\zeta = 0.50$ b. $\kappa = 1.00$

Fig. 5 Critical torque for which stall occurs ($\rho = 1.00$, $\gamma = 0$, $\delta = 5/6$, $\alpha_1 = 0$). In each panel the *shaded regions* correspond to parameter values for which stall does not occur

$\omega = 1$ [16]. Therefore, in the analytical work that follows we will assume that the applied torque α is constant within the resonance region, so that unless noted $\alpha_1 = 0$.

Shaft damage ($\kappa \neq 0$) In the presence of damage, with $\kappa \neq 0$, equilibrium points of (3), which correspond to stationary solutions of the original equations, can be determined from the roots of the equation

$$\rho^2 - 4\alpha_0\zeta = \left(\rho^2 - 2\alpha_0\kappa\delta\sin(2\gamma)\right)\cos(2p_{1,\mathrm{eq}}) - \left(2\alpha_0\kappa\delta\cos(2\gamma)\right)\sin(2p_{1,\mathrm{eq}}). \tag{6}$$

Once the equilibrium value of $p_{1,\mathrm{eq}}$ is known, the remaining states can be easily determined and in particular, $p_{2,\mathrm{eq}} = 0$, and $r_{1,\mathrm{eq}} = r_{2,\mathrm{eq}} = \alpha_0/(\rho\sin(p_{1,\mathrm{eq}}))$. By considering (3c, 3d) it is possible to show that no equilibria exist with $p_{2,\mathrm{eq}} = 0$ but $r_{1,\mathrm{eq}} \neq r_{2,\mathrm{eq}}$. Likewise, no equilibrium points exist with $r_{1,\mathrm{eq}} = r_{2,\mathrm{eq}}$ and $p_{2,\mathrm{eq}} \neq 0$. However, we note that other equilibria may possibly exist in the system with $p_{2,\mathrm{eq}} \neq 0$ and $r_{1,\mathrm{eq}} \neq r_{2,\mathrm{eq}}$, though none have been found.

Equation (6) has real solutions provided the following inequality is satisfied

$$\rho^4 - 4\rho^2\alpha_0\kappa\delta\sin(2\gamma) + (2\alpha_0\kappa\delta)^2 \geq \left(\rho^2 - 4\alpha_0\zeta\right)^2. \tag{7}$$

The bifurcation set of this system is identified as those parameter values for which the equality holds in (7). In general the value of α_0 may be solved as

$$\alpha_0 = 0, \quad \text{or} \quad \alpha_0 = \rho^2\frac{\kappa\delta\sin(2\gamma) - 2\zeta}{(\kappa\delta)^2 - (2\zeta)^2}. \tag{8}$$

In Fig. 5 the bifurcation set for this system is shown as both κ and ζ vary. In each figure the shaded regions of parameter space correspond to parameter values for which no equilibrium solutions occur in the averaged equations. In these results the equilibrium points that exist for $\alpha_0 < 0$ are unstable, so that the system cannot approach these states as time increases. As seen in Fig. 5a, as κ increases the interval of the torque (α_0) for which rotordynamic stall occurs increases. In contrast, as ζ increases, this torque interval shrinks. We note that the value of α_0 on the bifurcation set is singular for $2\zeta = \kappa\delta$. For $\kappa\delta > 2\zeta$ equilibria exist for any positive torque and in fact can exist for $\alpha_0 < 0$ as well. Finally, in Fig. 6, these bifurcation sets are presented as the parameters vary. In particular, as seen in Fig. 6c for varying γ, rotordynamic stall is more prevalent when the shaft crack lags the imbalance ($\gamma < 0$). Such trends are generally consistent with the numerical results of Sawicki et al. [13] in the presence of a breathing crack.

However, the existence of an equilibrium point of the averaged equations does not imply that all initial conditions are attracted to this stationary state. Instead, as illustrated in Fig. 3 for simulations of the original equations of motion, because of the strongly nonlinear structure of the system, the response depends on both parameter values and initial conditions. Numerically, it is found that capture into resonance occurs for large α_0 only occurs with significant initial vibration amplitudes—zero initial conditions pass through the resonance.

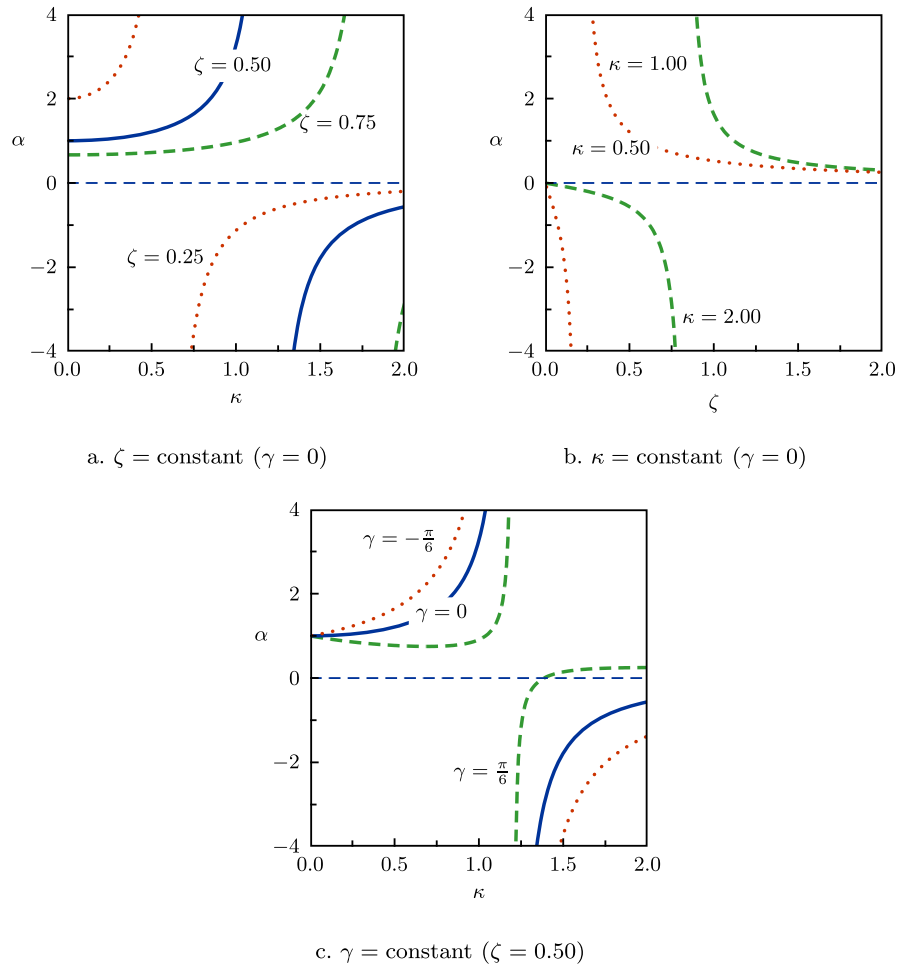

a. $\zeta =$ constant $(\gamma = 0)$ b. $\kappa =$ constant $(\gamma = 0)$

c. $\gamma =$ constant $(\zeta = 0.50)$

Fig. 6 Critical torque for which stall occurs ($\rho = 1.00$, $\delta = 5/6$, $\alpha_1 = 0$; cf. Fig. 5)

4 Capture into resonance

For $\varepsilon = 0$, the unperturbed averaged equations reduce to

$$\frac{dp_1}{dt} = w,$$

$$\frac{dw}{dt} = \alpha_0 - \rho\left[\frac{r_1}{2}\sin(p_1 + p_2) + \frac{r_2}{2}\sin(p_1 - p_2)\right],$$

$$\frac{dr_1}{dt} = 0,$$

$$\frac{dr_2}{dt} = 0,$$

$$\frac{dp_2}{dt} = 0,$$

so that r_1, r_2, and p_2 are constant in this limit and these equations are equivalent to a forced pendulum. In this limit a pair of equilibrium points exists for

$$\sqrt{r_1^2 + 2r_1 r_2 \cos(2p_2) + r_2^2} > \left|\frac{2\alpha_0}{\rho}\right|, \tag{9}$$

and the phase portrait of this reduced system is shown in Fig. 7. In particular, the system possesses a homoclinic orbit connecting the unstable equilibrium point to itself. Recall that $\mathcal{O}(1)$ values of the variable w correspond to solutions that are within the resonance region. Therefore, trajectories that lie in the interior of this homoclinic orbit remain within the resonance region for all time while trajectories outside of this region pass through the resonance region. If the above inequality is not satisfied the averaged system contains no equilibrium points and all trajectories pass through the resonance.

For $\varepsilon \neq 0$ the homoclinic orbit no longer exists. Instead, the stable and unstable manifolds of the sad-

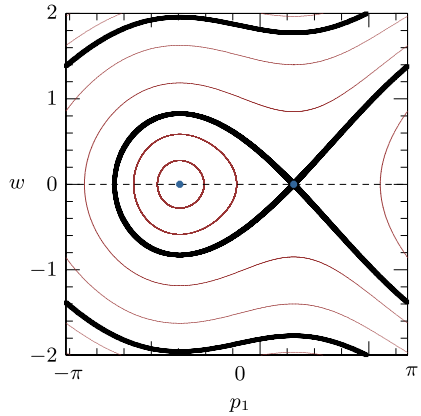

Fig. 7 Unperturbed phase portrait ($\alpha_0 = 0.25$, $\rho = 1.00$, $r_1 = r_2 = 0.50$, $p_2 = \pi/2$)

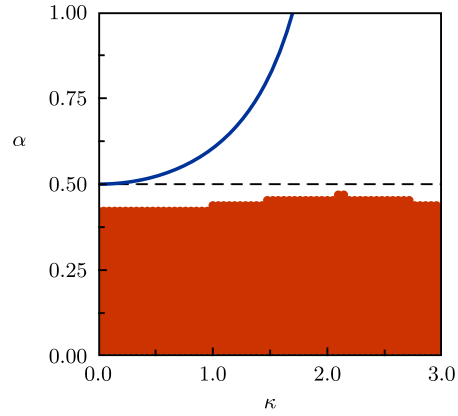

Fig. 8 Numerical simulation of (1) ($e\zeta = 0.10$, $e\rho = 0.10$, $\delta = 0.833$, $\gamma = 0$, $\alpha_1 = 0$, $d = 0.10$). For each marked parameter set (κ, α_0), the trajectory with zero initial conditions is captured

dle point split and allow for the possibility for trajectories that initially lie below the resonance region to become captured into resonance as they approach the resonance. Moreover, the variables r_1, r_2, and p_2, on which depends the existence of the homoclinic orbit, are no longer stationary.

However, since the evolutions of r_1, r_2, and p_2 are $\mathcal{O}(\varepsilon)$, the structure of phase space depends on the instantaneous values of these variables. Specifically, the region of phase space that corresponds to resonance capture exists provided the inequality in (9) is satisfied for the instantaneous values of the slowly varying parameters. As the system approaches the resonance the slowly-varying quantities r_1, r_2, and p_2 must take on values such that the resonance region exists, allowing trajectories to be captured into this region [18].

Away from the resonance the response of the system is quasi-stationary, so that amplitude of the translational oscillations in both the z and x coordinates can be approximated by the forced single-degree-of-freedom equations

$$\ddot{z} + 2(e\zeta)\dot{z} + z = d + e\rho\omega^2 \cos(\omega t),$$
$$\ddot{x} + 2(e\zeta)\dot{x} + x = e\rho\omega^2 \sin(\omega t).$$

Away from the resonance the values of r_1, r_2, and p_2 can be approximated from the averaged equations as

$$r_1 \sim \frac{e\rho}{\sqrt{(1-\omega^2)^2 + (2e\zeta\omega)^2}},$$
$$r_2 \sim \frac{e\rho}{\sqrt{(1-\omega^2)^2 + (2e\zeta\omega)^2}},$$
$$p_2 \sim 0.$$

Therefore, as the system approaches the resonance $\omega \to 1$ and

$$r_1 \sim \frac{\rho}{2\zeta}, \qquad r_2 \sim \frac{\rho}{2\zeta}, \qquad p_2 \sim 0.$$

Evaluating (9) for these instantaneous values, as the response approaches the resonance, the rotordynamic stall is expected to occur only provided

$$\alpha_0 < \frac{\rho^2}{2\zeta}, \tag{10}$$

which is identical to the condition for the existence of the equilibria in the undamaged shaft, although the above analysis also holds for $\kappa \neq 0$.

Returning to the original equations of motion, in Fig. 8 those values of α_0 and κ that lead to captured trajectories are shown when the system is integrated with zero initial conditions. In addition, the predicted parameter values which are expected to lead to resonance capture, from (10), is shown as the dashed line. Finally, the critical α_0 for which stationary solutions are expected to exist, corresponding to rotordynamic stall (cf. (8), is shown with the solid curve. The approximation from (10) clearly provides a better approximation to those parameter values that lead to capture from states that are initially well below the resonance, although such solutions may exist for specific initial conditions.

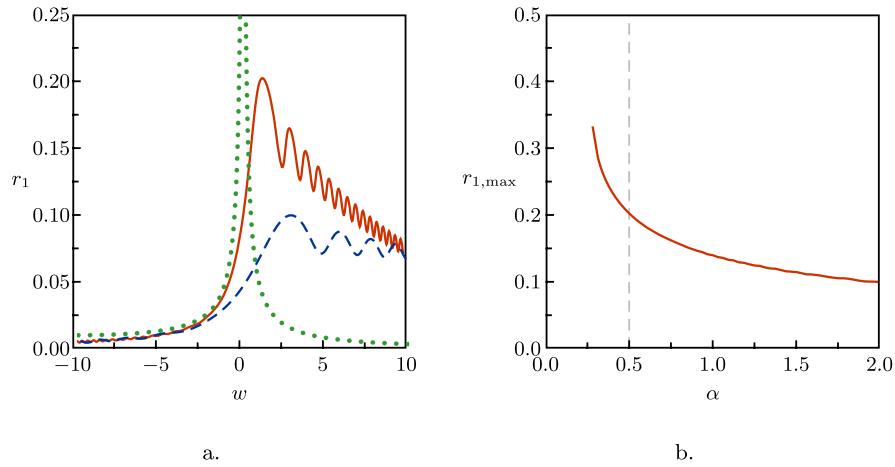

Fig. 9 Amplitude r_1 as the system passes through resonance ($\varepsilon = 0.10$, $\rho = 1$, $\kappa = 0$, $\alpha_1 = 0$); (**a**) r_1 vs. w; $\alpha_0 = 0.00$—*dotted line*, $\alpha_0 = 0.50$—*solid line*, $\alpha_0 = 2.00$—*dashed line*, (**b**) $r_{1,\max}$ vs. α_0

5 Passage through resonance

For initial conditions that pass through the resonance, the amplitude of the structural vibrations can still reach unacceptably large values due to the coupling between the rotational and translational motion. As shown above, as the system approaches the resonance from initial conditions below the resonance, we find from the previous analysis that $r_1 \sim r_2$ and $p_2 \sim 0$. With these restrictions, the averaged equations reduce to

$$\frac{dp_1}{dt} = w + \frac{\varepsilon}{2}\left\{\rho\frac{\cos p_1}{r_1} + \kappa\left[1 + \delta\cos\big(2(p_1+\gamma)\big)\right]\right\}, \tag{11a}$$

$$\frac{dw}{dt} = \alpha_0 - \rho r_1 \sin p_1, \tag{11b}$$

$$\frac{dr_1}{dt} = \varepsilon\left\{-\zeta r_1 + \rho\frac{\sin p_1}{2} + \frac{\kappa\delta}{2}\left[r_1\sin\big(2(p_1+\gamma)\big)\right]\right\}. \tag{11c}$$

The behavior of the system as it passes through the resonance can be approximated with these equations. As illustrated in Fig. 9a, if the system is initiated with $w(0) = -15$, which corresponds to an initial condition well below the resonance, as the system approaches the resonance near $w = 0$ the amplitude r_1 of the response grows before decaying as the system passes through the resonance. The dotted line represents the stationary amplitude obtained with $\alpha_0 = 0$. Notice that, as shown in Fig. 9a, as the external torque increase from $\alpha_0 = 0.50$ (solid) to $\alpha_0 = 2.00$ (dashed), the rotational component passes through the resonance more quickly and growth in the amplitude of the response is decreased. In Fig. 9b the maximum response amplitude as the system passes through the resonance is shown as α_0 varies. This maximum amplitude is only shown for solutions that pass through the resonance. For $\alpha_0 < 0.28$, the response is captured into resonance and the response instead approaches the amplitude described in Sect. 3.1. The dashed line indicates the critical value of α_0 below which stationary resonant solutions are expected to occur according to (10), $\alpha_0 < 0.50$ for these parameters. Between $\alpha_0 = 0.28$ and $\alpha_0 = 0.50$, such solutions occur, but the system is not captured into resonance with the initial conditions chosen well below the resonance.

6 Conclusions

The work has presented an analysis of capture and passage through resonance in a rotordynamic system, whereby a constant external torque is insufficient to drive the system through a critical speed due to the presence of a rotational imbalance. A generalized Jeffcott rotor model was presented, including stiffness anisotropy assumed to arise from shaft cracks, to describe this phenomena and the results were shown to be sensitive to both parametric variations and initial conditions. Using the method of averaging this model was reduced to a form described as a slowly-varying single-degree-of-freedom nonlinear oscillator. Equilibrium points of these averaged equations correspond to stationary solutions of the original equations, which imply the rotordynamic stall occurs. In addition, this

analysis is able to describe the role of the initial conditions and in particular the energy contained within the translational motion as the system approaches the resonance.

The equilibrium points of the averaged equations can be easily determined in the absence of damage and stall occurs for a limited range of external torque and damping. In the absence of damage, as the system is captured into resonance, the amplitude of the translational vibrations increases as $\sqrt{\alpha_0}$ while the frequency at which the rotor stalls increases up to the resonant frequency of the translational oscillations. From the averaged equations, the relationship between torque, damping, imbalance, and stiffness that leads to stalled solutions can be determined. In the presence of shaft cracks the interval of external torques over which stall occurs (for some initial conditions) increases dramatically. Considering the response of the system to zero initial conditions, modeling the transient spin-up of the unbalanced shaft, the averaged equations predict that the translational motion must be of sufficient amplitude for the region of sustained resonance to exist as the system approaches the resonance region. The anisotropy in the stiffness, characterized by the parameter κ, in general increases the values of the external torque over which a sustained resonant response can exist. However, the probability that a system will be captured into resonance when initiated well below the resonance region is seen to be relatively insensitive to the anisotropic stiffness.

Acknowledgements This material is based upon work supported by the National Science Foundation under Grant No. CMS–0201347. Any opinions, findings, and conclusions or recommendations expressed in this material are those of the author and do not necessarily reflect the views of the National Science Foundation.

References

1. Genta, G., Delprete, C.: Acceleration through critical speeds of an anisotropic, non-linear, torsionally stiff rotor with many degrees of freedom. J. Sound Vib. **180**(3), 369–386 (1995)
2. Ishida, Y., Yasuda, K., Murakami, S.: Nonstationary oscillation of a rotating shaft with nonlinear spring characteristics during acceleration through a major critical speed (a discussion by the asymptotic method and the complex-FFT method). J. Vib. Acoust. **119**(1), 31–36 (1997)
3. Wauer, J., Suherman, S.: Vibration suppression of rotating shafts passing through resonances by switching shaft stiffness. J. Vib. Acoust. **120**(1), 170–180 (1998)
4. Neishtadt, A.I.: Passage through a separatrix in a resonance problem with a slowly-varying parameter. J. Appl. Math. Mech. **39**(4), 594–605 (1975)
5. Rand, R.H., Kinsey, R.J., Mingori, D.L.: Dynamics of spinup through resonance. Int. J. Non-Linear Mech. **27**(3), 489–502 (1992)
6. Quinn, D.D., Rand, R.H., Bridge, J.: The dynamics of resonant capture. Nonlinear Dyn. **8**, 1–20 (1995)
7. Quinn, D.D.: Resonance capture in a three-degree-of-freedom mechanical system. Nonlinear Dyn. **14**, 309–333 (1997)
8. Dimentberg, M.F., McGovern, L., Norton, R.L., Chapdelaine, J., Harrison, R.: Dynamics of an unbalanced shaft interacting with a limited power supply. Nonlinear Dyn. **13**, 171–187 (1997)
9. Quinn, D.D.: Resonances in slowly varying dynamical systems. In: Sahu, A.R., Bhargava, R.R., Gupta, A.P. (eds.) Advances in Elastic Vibrations, Smart Structures, and Their Solution Technologies, pp. 1–10. Phoenix, New Delhi (2001)
10. Balthazar, J.M., Cheshankov, B.I., Ruschev, D.T., Barbanti, L., Weber, H.I.: Remarks on passage through resonance of a vibrating system with two degrees of freedom, excited by a non-ideal energy source. J. Sound Vib. **239**(5), 1075–1085 (2001)
11. Samantaray, A.K.: Steady-state dynamics of a non-ideal rotor with internal damping and gyroscopic effects. Nonlinear Dyn. (2008). doi:10.1007/s11071-008-9413-8
12. Gasch, R.: A survey of the dynamic behavior of a simple rotating shaft with a transverse crack. J. Sound Vib. **160**(2), 313–332 (1993)
13. Sawicki, J.T., Gyekenyesi, A.L., Baaklini, G.Y.: Analysis of transient response of cracked flexible rotor. In: Shull, P.J., Gyekenyesi, A.L. (eds.) Proceedings of SPIE, Int. Soc. Opt. Eng., vol. 5393, pp. 142–150 (2004)
14. Balthazar, J.M., Mook, D.T., Ingo, H., Brasil, R., Fenili, A., Belato, D., Felix, J.L.P.: An overview on non-ideal vibrations. Meccanica **38**, 613–621 (2003)
15. Bolla, M.R., Balthazar, J.M., Felix, J.L.P., Mook, D.T.: On an approximate analytical solution to a nonlinear vibrating problem, excited by a nonideal motor. Nonlinear Dyn. **50**, 841–847 (2007)
16. El-Badawy, A.A.: Behavioral investigation of a nonlinear nonideal vibrating system. J. Vib. Control **13**(2), 203–217 (2007)
17. Zniber, A., Quinn, D.D.: Resonance capture in a damped three-degree-of-freedom system: Experimental and analytical comparison. Int. J. Non-Linear Mech. **41**, 1128–1142 (2006)
18. Kath, W.L.: Necessary conditions for sustained reentry roll resonance. SIAM J. Appl. Math. **43**(2), 314–324 (1983)